THE CRYSTAL STRUCTURE OF ROSSITE

F. R. AHMED AND W. H. BARNES
Pure Physics Division, National Research Council, Ottawa, Canada

ABSTRACT

The crystal structure of rossite, $Ca(VO_3)_2.4H_2O$, has been determined from three-dimensional Patterson and Fourier syntheses employing 2729 observed reflections. The structure has been refined by two cycles of differential syntheses including corrections for finite summation errors. The final R-factor is 0.05_8 for the observed data. As in the lower hydrate, metarossite ($Ca(VO_3)_2.2H_2O$), the oxygen atoms are co-ordinated with V in the form of distorted trigonal bipyramids, and oxygen atoms and water molecules are co-ordinated with Ca in the form of distorted "square" antiprisms. Both in rossite and in metarossite the trigonal bipyramids share edges to form double chains. These chains in rossite, however, are cross-linked only through six shared corners to the calcium co-ordination polyhedra, which occur in pairs joined by a shared edge. Long hydrogen bonds from the water molecules serve as additional links between the two types of polyhedra.

INTRODUCTION

A determination of the structure of metarossite, $CaO.V_2O_5.2H_2O$, has been reported by Kelsey & Barnes (1960, 1961). The present investigation of rossite, $CaO.V_2O_5.4H_2O$, was undertaken in order to study the possible effects of the additional molecules of water on the oxygen co-ordination polyhedra around Ca and V, and on the linkages among them. Because rossite transforms slowly into metarossite under atmospheric conditions of low humidity, specimens of the former normally consist largely of the latter. Crystals of rossite, however, separate from aqueous solutions of rossite or of metarossite (Foshag & Hess, 1927). The material (Harvard No. 87328) employed in the present study came from Dolores River, Colorado, and was kindly supplied by Professor C. Frondel. A small amount of the powdered mineral was dissolved in hot water and allowed to crystallize by spontaneous slow evaporation at a temperature of about 21° C. The very small crystals of rossite so obtained were then employed to seed other solutions in order to obtain good crystals of reasonable dimensions. The prismatic specimen finally selected for the measurement of the unit cell parameters, and for the collection of intensity data, had a cross-section of 0.17 mm. × 0.08 mm. and a length of 0.20 mm. To avoid dehydration of the crystal before the collection of data had been completed, the experimental work was carried out during the humid summer months.

DATA COLLECTION

Zero-level precession photographs were employed for an examination of the quality of the reflections from various crystals and to obtain preliminary data on the size and shape of the unit cell. The crystal finally selected was then transferred to a diffractometer equipped with a scintillation counter and a single-crystal orienter. All data were collected with zirconium-filtered Mo radiation ($K\alpha_1$, $\lambda = 0.70926$ Å; $K\alpha_2$, $\lambda = 0.71354$ Å).

The unit cell parameters were measured with a narrow slit (0.02°) and a take-off angle of 1°. The 2θ positions of the $K\alpha_1$ and $K\alpha_2$ peaks of all observable medium- and high-order axial reflections were recorded together with the interaxial angles, and the final unit cell constants were taken as the arithmetical means of those deduced from the separate measurements. To facilitate direct comparison between the counter data and the preliminary precession photographs, the primitive cell selected at this stage was not the fully reduced one. It was transformed (Donnay & Nowacki, 1954) prior to the final calculation of structure factors.

The integrated intensities were measured at a take-off angle of 2° by the moving-crystal moving-counter method and fast scan (Furnas, 1957). The background count was recorded for each reflection and was subtracted from the total, and the results for all the reflections were reduced to the same relative scale (Bachmann, Ahmed & Barnes, 1961). The intensity data were modified by the $1/Lp$ factor for normal beam, but no absorption corrections were applied ($\mu \approx 29$ cm.$^{-1}$). Of 3744 possible reflections for which $(\sin \theta/\lambda) < 0.8$, 2610 (70%) were observed. This was increased to 2729 by the inclusion of 119 reflections measured during a partial scan over $(\sin \theta/\lambda) \geqq 0.8$.

CRYSTAL DATA

Rossite is triclinic, $P\bar{1}$, with a primitive reduced cell ($c < a < b$) of $a = 8.534$ Å, $b = 8.556$ Å, $c = 7.015$ Å ($\sigma \approx 0.005$ Å), and $\alpha = 101°32'$, $\beta = 114°58'$, $\gamma = 103°23'$ ($\sigma \approx 5'$); $V = 425.3$ Å^3, $F.W. = 310.04$, $Z = 2$, $D_c = 2.42$ gm./ml., $D_o = 2.45$ gm./ml. (Foshag & Hess, 1927). It is of interest to note that the volume of the unit cell of metarossite is 325.1 Å^3 ($Z = 2$), so that the apparent volume per molecule of H_2O is $(425.3–325.1)/4 = 25.0_5$ Å^3, compared with an estimate of about 25 Å^3 based on data for hewettite ($CaO.3V_2O_5.9H_2O$) and metahewettite ($CaO.3V_2O_5.3H_2O$), (Barnes & Qurashi, 1952, pp. 413, 415).

STRUCTURE DETERMINATION AND REFINEMENT

As in the case of metarossite (Kelsey & Barnes, 1960, p. 449) a three-dimensional sharpened Patterson synthesis revealed six prominent concentrations of high vector density in the asymmetric volume, thus indicating $P\bar{1}$, rather than $P1$, as the space group. There was no difficulty in identifying the maxima arising from the metal-metal interactions because they were in the ratios of 1.00:1.28:1.95 (calculated for Ca^{2+}–Ca^{2+}, Ca^{2+}–V, V–V; 1.00:1.28:1.63).

Structure factors calculated with the co-ordinates for the Ca and two V derived from the Patterson synthesis, and with $B = 1.2$ Å^2, showed $R = 0.40$ for all the observed reflections. A three-dimensional Fourier synthesis, computed with about 70 per cent of the observed data, produced electron-density maxima of 82 $e.\text{Å}^{-3}$ and 42 $e.\text{Å}^{-3}$ at the positions of the vanadium atoms and the calcium atom, respectively, and from 10 $e.\text{Å}^{-3}$ to 13 $e.\text{Å}^{-3}$ at thirteen other locations. Three of the last were rejected as possible O positions, partly on packing considerations and partly because they were very much sharper and different in shape from the remaining ten concentrations of electron density. These ten sites, therefore, were selected for the oxygen atoms. Structure factors calculated for the Ca, two V, and ten O, with $B = 1.0$ Å^2 for Ca and V, and $B = 2.0$ Å^2 for O, gave $R = 0.21$. A second three-dimensional Fourier synthesis, evaluated with about 97 per cent of the observed data, showed electron-density maxima of 100 $e.\text{Å}^{-3}$, 60 $e.\text{Å}^{-3}$, and 12 $e.\text{Å}^{-3}$ to 20 $e.\text{Å}^{-3}$ for the two vanadium atoms, the calcium atom, and the ten oxygen atoms, respectively, while they were < 3 $e.\text{Å}^{-3}$ at the three rejected locations. Structure factors calculated with the co-ordinates derived from this synthesis, and with $B = 0.9$ Å^2 for Ca and V, and with $B = 2.0$ Å^2 for O, showed a reduction of R to 0.15 for all the observed data.

Refinement of the structure was carried out by two cycles of differential syntheses with both the observed and calculated data. Corrections for the finite summation errors were made with the back-shift method (Booth, 1946). The isotropic temperature parameters were refined by comparison of the observed and calculated electron-density maxima and curvatures for the individual atoms, taking into account the overall modifications of the scale and temperature factors indicated by plots of $\log_e(\Sigma|F_c|/\Sigma|F_o|)$ against $\sin^2\theta$. The scattering factor curves employed throughout the investigation were those given by Freeman (1959) for V^{2+}, Ca^{2+}, and O^{1-}. The hydrogen atoms of the water molecules were not included in any of the structure-factor calculations although some reasonably clear indications of the sites of most of them appeared in a final three-dimensional difference synthesis. The final R-factor was 0.05_8 for all the observed reflections; it was 0.06_2, 0.05_4, and 0.06_1 for the observed $0kl$, $h0l$, and $hk0$ reflections, respectively.

RESULTS

The final fractional atomic co-ordinates, referred to the primitive reduced cell, are given in Table 1 together with their estimated standard

TABLE 1. FRACTIONAL CO-ORDINATES OF THE ATOMS AND THEIR E.S.D.'S, ASSUMING THE ATOMS TO BE SPHERICAL.
(All atoms in equipoints x,y,z and $\bar{x},\bar{y},\bar{z}$)

Atom	x	y	z	σ(Å)
Ca	0.8390	0.1503	0.9927	0.0007
V_1	0.4358	0.3328	0.8002	0.0006
V_2	0.3783	0.3366	0.2756	0.0006
O_1	0.4720	0.4142	0.0992	0.0038
O_2	0.4967	0.3835	0.5833	0.0030
O_3	0.8042	0.2731	0.6976	0.0040
O_4	0.1625	0.3207	0.1785	0.0035
O_5	0.2119	0.2315	0.6576	0.0038
O_6	0.5357	0.1903	0.8434	0.0035
O_7	0.3741	0.1385	0.1984	0.0033
O_8	0.9848	0.0108	0.7775	0.0033
O_9	0.7195	0.1162	0.2533	0.0035
O_{10}	0.8948	0.4398	0.2072	0.0067

deviations obtained from the expression, $\sigma(x) \sim (R/\bar{s})(N/8p)^{\frac{1}{2}}$ (Cruickshank, 1960), assuming the atoms to be nearly spherical. It may be noted that these e.s.d.'s are from 20 per cent to 40 per cent higher than corresponding ones calculated with expression (12) of the *International Tables* (1959) or with expression (**b**) of Table 288 given by Lipson & Cochran (1953). The observed and calculated electron densities, the mean curvatures at the atomic positions, and the final isotropic temperature parameters are listed in Table 2. Not evident from this table is the fact that O_1, O_3, O_4, and O_{10} showed some evidence of anisotropic thermal motion although they were treated isotropically. To conserve space a complete list of observed structure amplitudes and calculated structure

TABLE 2. OBSERVED AND CALCULATED ELECTRON DENSITIES (e.Å^{-3}), MEAN CURVATURES (e.Å^{-5}), AND ASSUMED ISOTROPIC TEMPERATURE PARAMETERS (Å^2)

Atom	$\rho_{obs.}$	$\rho_{calc.}$	$-\rho_{obs.}''$	$-\rho_{calc.}''$	B
Ca	101.7	105.8	1772	1888	0.80
V_1	130.7	132.5	2346	2377	0.72
V_2	132.1	133.5	2395	2406	0.72
O_1	25.0	23.9	353	339	1.67
O_2	28.3	27.9	452	441	0.97
O_3	22.2	22.4	301	315	1.79
O_4	25.3	26.8	405	434	1.43
O_5	23.2	23.2	356	353	1.67
O_6	25.8	26.6	379	405	1.43
O_7	27.6	27.0	443	437	1.28
O_8	26.1	25.8	405	401	1.28
O_9	24.0	23.2	333	324	1.67
O_{10}	15.7	16.4	177	199	3.28

factors is not given, but an agreement summary for all the data (see Hanson & Ahmed, 1958) is presented in Table 3. The observed structure amplitudes varied from 4.2 to 109.8 and $F(000) = 308$.

TABLE 3. AGREEMENT SUMMARY

Observed reflections		
	Category	Number
(1)	$\lvert\Delta F\rvert \leq 4.2$, *or*, $\lvert\Delta F\rvert \leq 0.12F_o$	2710
(2)	$\lvert\Delta F\rvert \leq 8.4$, *or*, $\lvert\Delta F\rvert \leq 0.18F_o$	19
(3)	$\lvert\Delta F\rvert \leq 12.6$, *or*, $\lvert\Delta F\rvert \leq 0.24F_o$	0
	Total	2729

Unobserved reflections		
	Category	Number
(1)	$\lvert F_c\rvert \leq 1.5F_{th}$	1130
(2)	$1.5F_{th} < \lvert F_c\rvert \leq 3.0F_{th}$	2
(3)	$\lvert F_c\rvert > 3.0F_{th}$	2
	Total	1134

NOTES. F_{th} = threshold value; $\lvert\Delta F\rvert = \lvert\,\lvert F_o\rvert - \lvert F_c\rvert\,\rvert$; each category includes all reflections which meet the specified conditions, and which have not been included previously; category (3) for the Unobserved Reflections was traced back to an error in the φ-angles for the two reflections concerned.

DISCUSSION[1]

The setting for the unit cell of metarossite ($c > b > a$) was chosen for direct comparison with that of the unit cell of metahewettite (Barnes & Qurashi, 1952), later identified as the sodium analogue (Barnes, 1955), which is monoclinic with $a = 12.18$ Å, b (unique) $= 3.61_4$ Å, $c = 7.80$ Å, $\beta = 95.0°$ (Barnes & Qurashi, 1952; Qurashi, 1962), and it was retained for the investigation of the crystal structure of metarossite (Kelsey & Barnes, 1960). In order to facilitate discussion of the structures of rossite and metarossite, however, it is more convenient to select a new cell for rossite with contents more readily comparable with those of the cell previously chosen for metarossite. This is readily achieved by interchanging the b and c axes of rossite, reversing the direction of the new b axis (to retain a right-handed system of axes), and then transferring the origin to $0,\bar{1},0$. The new cell has $a = 8.534$ Å, $b = 7.015$ Å, $c = 8.556$ Å, $\alpha = 78°28'$, $\beta = 103°23'$, $\gamma = 65°02'$. The fractional co-ordinates in the

---

[1] Throughout the text of the Discussion, and in Tables 5, 6, 7, and 8, an asterisk denotes an atom in a cell adjacent to the reference cell outlined in the projections of Figs. 1 & 2. In the text, tables, and figures a prime without an asterisk identifies a centrosymmetrically located atom (within the reference cell) which is equivalent to one of those whose fractional co-ordinates are listed in Table 4.

new cell may be derived from those (Table 1) in the original cell as follows: x(new) = x(old), y(new) = 1-z(old), z(new) = y(old); they are listed in Table 4, together with the corresponding ones of Kelsey & Barnes (1960, Table 1) for metarossite. Throughout the remainder of the discussion all references are to the new unit cell for rossite, two axial projections of which are reproduced in Figs. 1 and 2.

TABLE 4. FRACTIONAL ATOMIC CO-ORDINATES REFERRED TO A CELL DIRECTLY COMPARABLE WITH THAT OF METAROSSITE

	rossite			metarossite		
Atom	x	y	z	x	y	z
Ca	0.8390	0.0073	0.1503	0.7595	0.4665	0.1470
V_1	0.4358	0.1998	0.3328	0.4485	0.1020	0.3360
V_2	0.3783	0.7244	0.3366	0.3750	0.5830	0.3450
O_1	0.4720	0.9008	0.4142	0.3915	0.8400	0.4170
O_2	0.4967	0.4167	0.3835	0.5170	0.3920	0.3835
O_3	0.8042	0.3024	0.2731	0.8610	0.7555	0.3655
O_4	0.1625	0.8215	0.3207	0.1050	0.4730	0.3345
O_5	0.2119	0.3424	0.2315	0.1930	0.0635	0.2350
O_6	0.5357	0.1566	0.1903	0.6245	0.1170	0.1870
O_7	0.3741	0.8016	0.1385	0.4300	0.6000	0.1460
O_8	0.9848	0.2225	0.0108	1.0070	0.7210	0.0130*
O_9	0.7195	0.7467	0.1162	—	—	—
O_{10}	0.8948	0.7928	0.4398	—	—	—

In Table 1 of Kelsey & Barnes (1960) the O_8 label was applied to the atom with $x = 0.0070$ in order to keep the co-ordinates of all reference atoms of the asymmetric unit within the unit cell. Therefore, in the present discussion, O_8 of rossite corresponds to O_8 of metarossite.

In rossite, as in metarossite, each calcium atom is co-ordinated with eight oxygen atoms which take the form of a distorted square antiprism. Similar co-ordination also occurs in conichalcite, $CaCu(AsO_4)(OH)$, (Qurashi & Barnes, 1963). In rossite the Ca–O distances in the $CaO_3(H_2O)_5$ antiprisms vary from 2.40 Å to 2.61 Å (mean, 2.48 Å), in metarossite these distances in the $CaO_5(H_2O)_3$ antiprisms vary from 2.40 Å to 2.59 Å (mean, 2.46 Å), while in conichalcite the Ca–O distances in the $CaO_7(OH)$ antiprisms vary from 2.36 Å to 2.68 Å (mean, 2.51 Å). Each of the two non-equivalent vanadium atoms in both rossite and metarossite is co-ordinated with five oxygen atoms which take the form of a distorted trigonal bipyramid.

There is no difficulty in equating Ca, V_1, V_2, O_1, O_2, O_4, O_5, O_7, and O_8 to corresponding atoms in the structures of rossite and metarossite (compare the present Figs. 1 and 2 with Figs. 4 and 5 of Kelsey & Barnes, 1960, pp. 456, 457, respectively). Furthermore, O_6 joins Ca to V_1, and O_5 is bonded only to V_1 in both structures, thus establishing their respective identities, although it may be noted in Table 4 that $y(O_5) < y(O_6)$ in

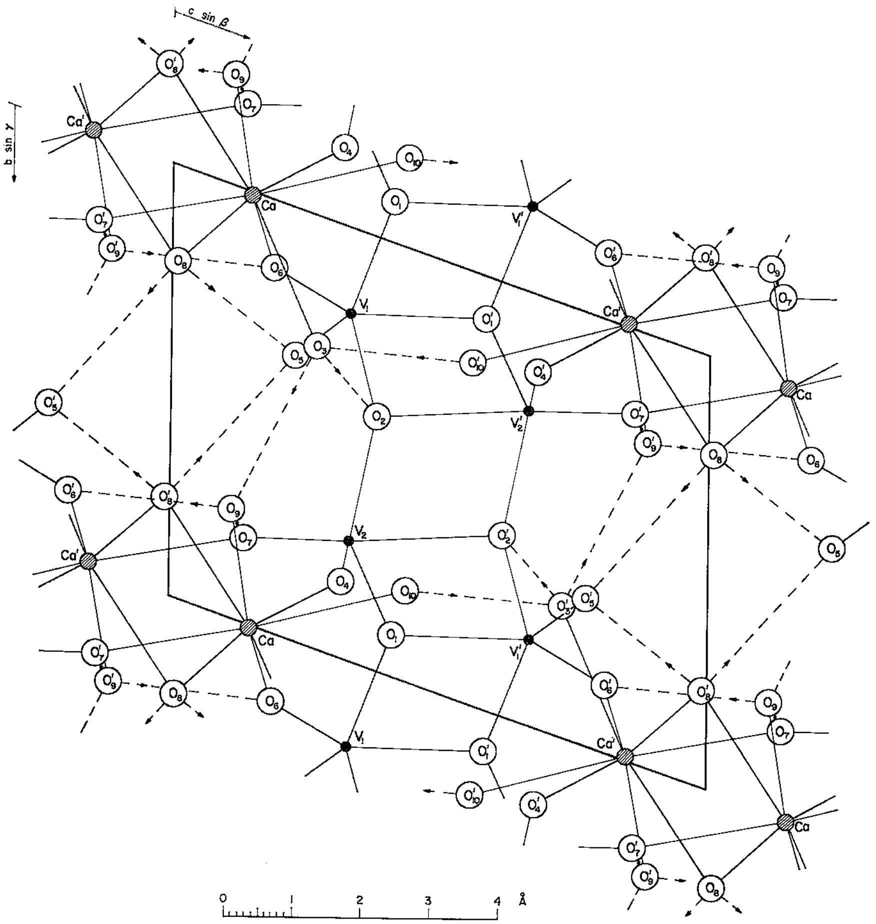

FIG. 1. Projection of the structure along [100]. Broken lines indicate long hydrogen bonds; arrowheads point away from H_2O molecules.

metarossite, but that $y(O_5) > y(O_6)$ in rossite. This has the effect of interchanging some of the specific interatomic distances, and particularly the angles, involving O_5 and O_6 (compare the present Tables 5 and 6 with Tables 3 and 4 of Kelsey & Barnes, 1960, pp. 458, 459 and 1961, p. 697). Of the remaining three oxygen atoms in rossite, two (O_9, O_{10}) must represent the additional water molecules and the third must correspond to O_8 in metarossite. The choice of labels for O_3, O_9, O_{10} (see Fig. 2) may be made on the basis of the Ca-antiprisms in rossite and metarossite. There is only one logical way in which to select the "square" faces of the antiprisms in metarossite because O_2, O_6, $O_7'^*$, O_7 are the only four atoms

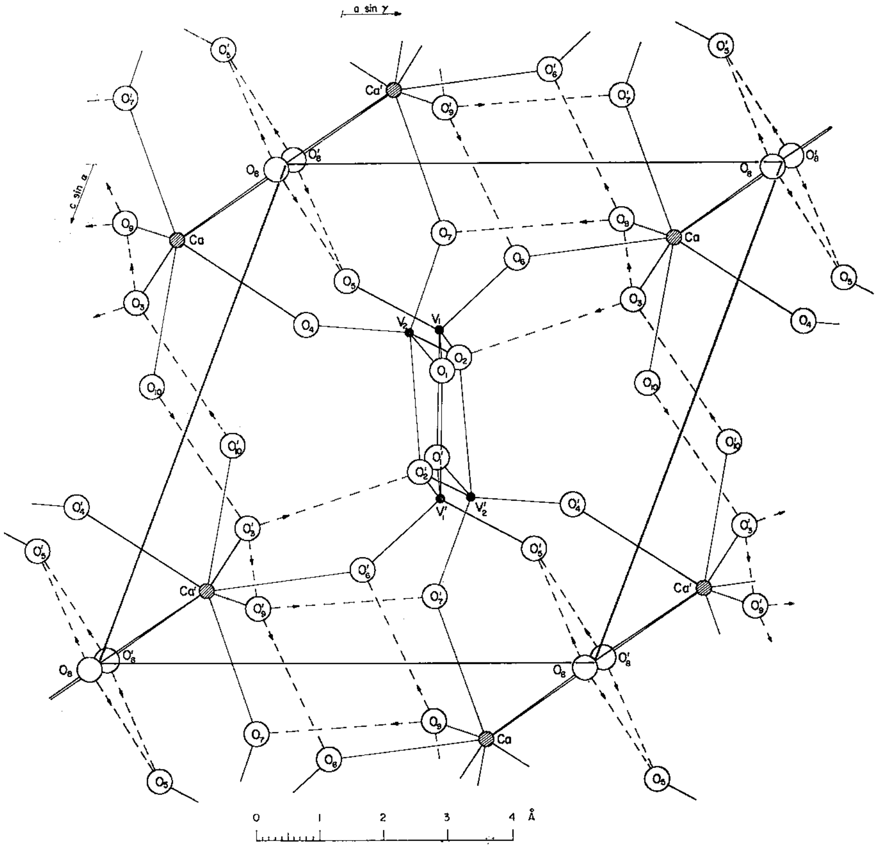

FIG. 2. Projection of the structure along [010]. Broken lines indicate long hydrogen bonds; arrowheads point away from H_2O molecules.

in the oxygen polyhedron which are virtually co-planar (see Kelsey & Barnes, 1960, Fig. 6C, where C.a should read Ca) and, therefore, must be the corners of one face. The other face is defined by O_3, $O_4{}^*$, $O_8{}'^*$, $O_8{}^*$, the mean plane of which is approximately parallel to the first and has been rotated approximately 45° about an axis nearly normal to both faces, but $O_4{}^*$ and $O_8{}^*$ are displaced from the mean plane away from the other face while O_3 and $O_8{}'^*$ are displaced in the direction of the other face. In the corresponding antiprisms of rossite, $O_{10}{}^*$ has replaced O_2, O_6 occupies the approximate site of O_7 which has been removed, and $O_9{}^*$ has replaced O_6. The mean planes of the two faces $O_{10}{}^*$, $O_9{}^*$, $O_7{}'^*$, O_6 and O_3, $O_4{}^*$, $O_8{}'^*$, $O_8{}^*$ are roughly parallel, and have been rotated approximately 45° relative to each other, like the corresponding planes in metarossite. The face

TABLE 5. INTERATOMIC DISTANCES (Å) IN THE CO-ORDINATION POLYHEDRA. (Parentheses indicate edges shared between two V-bipyramids or two Ca-antiprisms)

	O_1'	O_1^*	O_2	O_5	O_6
V_1	1.984	1.936	1.898	1.636	1.648
O_1'		(2.318)	(2.402)	3.105	3.346
O_1^*				2.760	2.668
O_2				2.783	2.668
O_5					2.656

	O_2'	O_1	O_2	O_4	O_7
V_2	2.198	1.879	1.862	1.632	1.660
O_2'		(2.402)	(2.506)	2.908	3.777
O_1				2.892	2.642
O_2				2.886	2.668
O_4					2.624

	O_{10}^*	$O_7'^*$	O_9^*	O_6	O_3	$O_8'^*$	O_4^*	O_8
Ca	2.446	2.397	2.473	2.486	2.444	2.561	2.405	2.609
O_{10}^*			2.976	2.941	3.245		2.772	
$O_7'^*$			3.118	3.075		3.114		3.123
O_9^*						3.038	4.075	
O_6					2.884			4.604
O_3							3.326	3.017
$O_8'^*$							2.958	(3.068)

The e.s.d.'s of the interatomic distances are 0.003 Å to 0.006 Å in the V-bipyramids, and 0.004 Å to 0.008 Å in the Ca-antiprism.

O_3, O_4^*, $O_8'^*$, O_8^* shows the same puckered type of distortion as the corresponding one in metarossite, but O_{10}^*, O_9^*, $O_7'^*$, O_6 are no longer virtually co-planar; O_{10}^* and $O_7'^*$ are displaced from the mean plane towards the other face, while O_9^* and O_6 are displaced in the opposite direction. If the O_3 label were to be interchanged with that of O_9, or that of O_{10}, the close resemblance between the antiprisms in rossite and metarossite would be destroyed. For this reason the designation of O_3 in the tables and figures was adopted. It may be noted in Table 4 that the co-ordinates of O_3 in metarossite are closer to those of the present O_{10} in rossite, but the largest difference between the present O_3 of rossite and O_3 of metarossite is in the *y* co-ordinate. However, this co-ordinate for Ca and all other oxygen atoms of the antiprism (with the exception of O_6) is of the same order of magnitude greater in metarossite as is that of the atom designated as O_3. Finally, it should be mentioned that a less distorted antiprism, with more nearly planar faces, could be selected in rossite by the choice of O_{10}^*, O_4^*, O_9^*, $O_8'^*$ and O_3, O_6, O_8, O_7 to define the "square" faces, but the equivalent polyhedron in metarossite bears

TABLE 6. BOND ANGLES (°) IN THE VANADIUM AND CALCIUM POLYHEDRA

O_1^*—V_1—O_1'	72.5	O_1—V_2—O_2'	71.7
O_2—V_1—O_1'	76.4	O_2—V_2—O_2'	75.7
O_1^*—V_1—O_5	100.9	O_1—V_2—O_7	96.4
O_1^*—V_1—O_6	95.9	O_1—V_2—O_4	110.8
O_2—V_1—O_5	103.7	O_2—V_2—O_7	98.3
O_2—V_1—O_6	97.4	O_2—V_2—O_4	111.2
O_1'—V_1—O_5	117.8	O_2'—V_2—O_7	156.3
O_1'—V_1—O_6	134.0	O_2'—V_2—O_4	97.7
O_5—V_1—O_6	107.9	O_7—V_2—O_4	105.7
O_1^*—V_1—O_2	146.8	O_1—V_2—O_2	129.3

O_{10}^*—Ca—O_9^*	74.4	$O_7'^*$—Ca—$O_8'^*$	77.7
O_{10}^*—Ca—O_6	73.2	$O_7'^*$—Ca—O_8	77.1
$O_7'^*$—Ca—O_9^*	79.6	O_3—Ca—O_6	71.6
$O_7'^*$—Ca—O_6	78.0	$O_8'^*$—Ca—O_9^*	74.2
O_3—Ca—O_4^*	86.6	O_6—Ca—O_8	129.3
O_3—Ca—O_8	73.2	O_9^*—Ca—O_4^*	113.3
$O_8'^*$—Ca—O_4^*	73.0	O_{10}^*—Ca—O_8	136.1
$O_8'^*$—Ca—O_8	72.8	O_{10}^*—Ca—$O_8'^*$	115.0
O_{10}^*—Ca—$O_7'^*$	145.9	$O_7'^*$—Ca—O_3	104.9
O_9^*—Ca—O_6	72.1	$O_7'^*$—Ca—O_4^*	142.6
O_3—Ca—$O_8'^*$	144.3	O_6—Ca—$O_8'^*$	141.3
O_4^*—Ca—O_8	72.4	O_6—Ca—O_4^*	138.8
O_{10}^*—Ca—O_3	83.1	O_9^*—Ca—O_3	141.4
O_{10}^*—Ca—O_4^*	69.7	O_9^*—Ca—O_8	142.8

The e.s.d.'s are 0.2° to 0.3° for angles O—V—O, and 0.3° to 0.4° for angles O—Ca—O. Note that in the rossite Ca-antiprism O_{10}^* has replaced O_2, O_9^* has replaced O_6, O_6 has replaced O_7, and O_8 is O_8^*, in metarossite.

no resemblance whatsoever to a square antiprism even if the label of O_3 is interchanged with that of O_9 or that of O_{10}. The interatomic distances and angles in the square antiprismatic co-ordination polyhedron of O around Ca in rossite are collected in Tables 5 and 6; the puckered configuration of both faces of the antiprism gives rise to the very long O_9^*–O_4^*, O_6–O_8 edges compared with the corresponding O_6–O_4^*, O_7–O_8^* edges in metarossite.

The Ca-antiprisms share the two edges O_7–$O_7'^*$ and O_8^*–$O_8'^*$ in metarossite to form double chains of Ca and Ca′ antiprisms along [100]. In rossite, however, only the edge O_8–$O_8'^*$ is shared so that the Ca and Ca′ antiprisms occur in isolated pairs; the Ca to Ca′ distance across the shared edge is 4.16 Å. Although the shared edge, O_8–$O_8'^*$, is no shorter than some others of the antiprism, the Ca is displaced away from this edge so that Ca–O_8 and Ca–$O_8'^*$ are significantly longer than the other Ca–O distances.

The trigonal bipyramidal co-ordination polyhedra of oxygen atoms around the two non-equivalent vanadium atoms, V_1 and V_2, are very nearly the same in both rossite and metarossite so that their detailed description in the latter (Kelsey & Barnes, 1960) applies equally well to the present structure. They are directly comparable with those in vanadium pentoxide (Bachmann, Ahmed & Barnes, 1961) and in various other structures containing pentavalent vanadium (Bachmann & Barnes, 1961). The bipyramids share their apices, O_1 and O_2, to form zigzag chains parallel to [010], which are linked into double chains with those symmetrically related through the centre at $\frac{1}{2},\frac{1}{2},\frac{1}{2}$ by the shared edges, $O_1{}^*$–$O_1{}'$, $O_1{}'$–O_2, O_2–$O_2{}'$, $O_2{}'$–O_1 (see Fig. 1). The interatomic distances and angles in the bipyramids of rossite are collected in Tables 5 and 6. As in metarossite, the shared edges are the shortest in these polyhedra, and V_1 and V_2 are displaced away from them, so that V_1–$O_1{}'$ and V_2–$O_2{}'$ are the longest V–O distances, and the apices of the bipyramids make acute angles (72°, 76°) with these long bonds. The V–V separations across the shared edges in rossite are $V_1{}'^*$ to V_1 = 3.16 Å, V_1 to $V_2{}'$ = 3.17 Å, $V_2{}'$ to V_2 = 3.21 Å, V_2 to $V_1{}'$ = 3.17 Å, compared with values of 3.08 Å to 3.16 Å in metarossite. These are shorter than the separations across the shared corners, namely, V_1 to V_2 (across O_2) = 3.51 Å, V_2–$V_1{}^*$ (across O_1) = 3.56 Å, compared with 3.55 Å and 3.58 Å, respectively, in metarossite. The displacements of V_1 and V_2 from the equatorial planes of the bipyramids ($O_1{}'$, O_5, O_6; $O_2{}'$, O_4, O_7) are both 0.04 Å in rossite and 0.06 Å in metarossite. The latter was not considered to be significant (Kelsey & Barnes, 1960) but the higher degree of accuracy attained in the present three-dimensional study of the rossite structure suggests that the vanadium atoms may not lie exactly in the equatorial planes.

In metarossite, the double chains of V-bipyramids are cross-linked to the double chains of Ca-antiprisms by the shared edge, O_2–O_6, between Ca and V_1, and by O_2–O_7 between Ca and V_2, on one side, and by the symmetrically equivalent $O_2{}'$–$O_6{}'$, between Ca′ and $V_1{}'$, and $O_2{}'$–$O_7{}'$, between Ca′ and $V_2{}'$, on the other side (see Kelsey & Barnes, 1960, Fig. 4). In addition they are joined to the antiprisms by the shared corners O_4 and O_7 between V_2, and Ca* and Ca′*, respectively, and by $O_4{}'$ and $O_7{}'$ between $V_2{}'$, and Ca′* and Ca*, respectively, separated by *c* along [001] (see Kelsey & Barnes, 1960, Fig. 5). In rossite, however, there are no shared edges between the V and Ca co-ordination polyhedra; cross-linkage occurs only through the shared corners O_4, O_6, O_7, $O_4{}'$, $O_6{}'$, $O_7{}'$ (see Fig. 2). The V to Ca distances across these shared corners are Ca* to V_2 (Ca′* to $V_2{}'$) = 3.91 Å, Ca to V_1 (Ca′ to $V_1{}'$) = 3.94 Å, Ca′* to V_2 (Ca* to $V_2{}'$) = 3.83 Å, compared with 3.25 Å and 3.30 Å across shared edges and 3.79 Å and 3.80 Å across shared corners in metarossite.

The Water Molecules

Reasons for the identification of O_3 and O_8 as water molecules have been given in connection with a discussion of the structure of metarossite (Kelsey & Barnes, 1960, pp. 459–462). The atoms O_9 and O_{10}, which are not present in metarossite, must represent the two additional molecules of water per formula unit in rossite. It may also be noted that O_3, O_8, O_9, and O_{10} are the only oxygen atoms associated only with the cation, Ca^{2+}, thus O_1 is co-ordinated with $V_1{}^*$, $V_1{}'$ and V_2, O_2 with V_1, V_2, and $V_2{}'$, O_3 with Ca only, O_4 with V_2 and Ca*, O_5 with V_1, O_6 with V_1 and Ca, O_7 with V_2 and Ca′*, O_8 with Ca and Ca′*, O_9 with Ca* only, and O_{10} with Ca* only. Furthermore, V_1–O_5, V_1–O_6, V_2–O_4, V_2–O_7 are very short (about 1.65 Å) and probably involve an appreciable proportion of double bond character (Bachmann & Barnes, 1961).

Apart from some of the O–O edges of the co-ordination polyhedra (Table 5) and one of the diagonals of each of the "square" faces of the antiprisms (O_9–$O_6{}^*$ = 2.92 Å, O_8–$O_4{}^*$ = 2.97 Å), there are no distances between oxygen atoms of less than 3.24 Å, with the exception of seven involving O_3, O_8, O_9, and O_{10}. These are O_3–O_2 = 2.84 Å, O_3–O_9 = 2.83 Å, O_3–$O_{10}{}'^*$ = 2.84 Å, O_8–$O_5{}^*$ = 2.89 Å, O_8–$O_5{}'^*$ = 2.82 Å, O_9–$O_6{}'^*$ = 2.74 Å, and O_9–O_7 = 2.86 Å, all of which are suggestive of long H-bonds.

Considering the environment of each H_2O molecule in turn, O_3 is surrounded by O_2, O_9, Ca, and $O_{10}{}'^*$ in a distorted tetrahedral array with the angles shown in Table 7. Furthermore, the final difference map shows residual electron density concentration maxima of about 0.7 $e.Å^{-3}$ on lines joining the site of O_3 with those of O_2 and O_9 and much closer to O_3 in both cases. There seems to be no doubt, therefore, that O_3 forms long H-bonds to O_2 and O_9 ($O_2 \cdots H \cdot O_3 \cdot H \cdots O_9$). A similar distorted tetrahedral arrangement of $O_5{}^*$, $O_5{}'^*$, Ca, and Ca′*, with the angles given in Table 7, surrounds O_8, and obviously involves the same system of H-bonds as occurs in metarossite ($O_5{}^* \cdots H \cdot O_8 \cdot H \cdots O_5{}'^*$). Confirmation again comes from the final difference synthesis where maximum residual electron-density concentrations of 0.7 $e.Å^{-3}$ to 0.8 $e.Å^{-3}$ occur on the lines joining the site of O_8 with those of $O_5{}^*$ and $O_5{}'^*$ and are much closer to O_8. In the case of O_{10}, the only close neighbours are Ca* and $O_3{}'^*$ and the angle Ca–O_{10}–$O_3{}'^*$ = 122.5°. Unfortunately the possible presence of an electron-density maximum, suggestive of a possible H between O_{10} and $O_3{}'^*$, in the final difference synthesis is largely obscured by positive and negative residual concentrations of electron density at the site of

TABLE 7. ANGLES (°) IN THE O_3 AND O_8 TETRAHEDRA. (Arrowheads indicate directions of long hydrogen bonds)

$O_2 \leftarrow O_3 \rightarrow O_9$	96.1	$O_5{}^* \leftarrow O_8 \rightarrow O_5{}'^*$	91.6
$O_2 \leftarrow O_3$—Ca	109.3	$O_5{}^* \leftarrow O_8$—Ca	91.6
$O_2 \leftarrow O_3 \leftarrow O_{10}{}'^*$	105.4	$O_5{}^* \leftarrow O_8$—Ca′*	111.5
$O_{10}{}'^* \rightarrow O_3 \rightarrow O_9$	95.2	Ca—$O_8 \rightarrow O_5{}'^*$	125.8
$O_{10}{}'^* \rightarrow O_3$—Ca	117.3	Ca′*—$O_8 \rightarrow O_5{}'^*$	101.9
Ca—$O_3 \rightarrow O_9$	129.7	Ca—O_8—Ca′*	107.2
mean	108.8	mean	104.9

O_{10} indicative of thermal anisotropy. It may be significant, however, that a small concentration of electron density (max. $\sim 0.4\ e.\text{Å}^{-3}$) appears in the difference map at approximately the expected distance from the site of O_{10} and close to the line joining the latter to the site of $O_3'^*$. It is probable, therefore, that a long H-bond exists between O_{10} and $O_3'^*$ ($O_{10}\cdot H\cdots O_3'^*$) but that the second H of O_{10} is not utilized in bond formation.

The question of O_9 is less certain. It is surrounded by O_3, O_7, $O_6'^*$, and Ca* with the angles shown in Table 8. There appears to be little doubt that a H-bond exists between O_9 and $O_6'^*$ ($O_9\cdot H\cdots O_6'^*$); O_9–$O_6'^* = 2.74$ Å, Ca*–O_9–$O_6'^* = 119.1°$, and there is a maximum residual electron-density concentration of about $0.8\ e.\text{Å}^{-3}$ in the final difference map close to the site of O_9 and to a line joining the sites of O_9 and $O_6'^*$. In the case of O_9 to O_7, however, the angle O_7–O_9–$O_6'^*$ is only 66.6°. Nevertheless, O_9–$O_7 = 2.86$ Å, and there is a suggestive residual electron-density concentration maximum of about $0.6\ e.\text{Å}^{-3}$ in the difference map. This maximum is at approximately the appropriate distance from O_9 to represent the H atom and it is slightly off the line joining the sites of O_9 and O_7 which, if real, would increase the H–O_9–H angle from 66.6° to more than 90°, because the H atom between O_9 and $O_6'^*$ also appears to be off the O_9–$O_6'^*$ line in the opposite direction. It is possible, therefore, that O_9 is H-bonded to both $O_6'^*$ and to O_7 ($O_7\cdots H\cdot O_9\cdot H\cdots O_6'^*$), as indicated in Figs. 1 and 2.

TABLE 8. ANGLES (°) IN THE DISTORTED TETRAHEDRON AROUND O_9. (Arrowheads indicate directions of probable long hydrogen bonds)

$Ca^*\text{—}O_9\rightarrow O_6'^*$	119.1
$Ca^*\text{—}O_9\rightarrow O_7$	125.5
$Ca^*\text{—}O_9\leftarrow O_3$	140.6
$O_7\leftarrow O_9\rightarrow O_6'^*$	66.6
$O_7\leftarrow O_9\leftarrow O_3$	77.2
$O_3\rightarrow O_9\rightarrow O_6'^*$	99.0
mean	104.7

Briefly the addition of the two water molecules, represented by O_9 and O_{10}, has had the following effects on the structure of metarossite. Each Ca-antiprism has been shifted relative to V_1 and V_2 by approximately $b/2$ in the y direction, with the exception of O_6, which has been transferred from one antiprism to the adjacent one along y and has been replaced in the original antiprism by O_9^*. The Ca–O_7 bond has been broken and O_6 has replaced O_7. The Ca–O_2 bond also has been broken and O_2 has been replaced by O_{10}^*. The Ca-antiprisms now share only one edge, O_8–$O_8'^*$, in isolated pairs, and are cross-linked to the double chains of V-bipyramids through corners only. While O_8 remains H-bonded to O_5^* and $O_5'^*$, O_8 is now H-bonded to O_2 and O_9, and the new water molecules have formed additional H-bonds, O_{10} to $O_3'^*$, and O_9 to $O_6'^*$ and (possibly) to O_7.

Grateful acknowledgment is made to Miss C. P. Saunderson for assistance with the data collection and the interpretation of the Patterson synthesis during the summer of 1960. Computations were carried out on IBM 650 computers with programmes written in this laboratory (Ahmed, 1961), and thanks are due to Mrs. M. E. Pippy for much assistance with desk calculations and with the operation of the computers.

REFERENCES

AHMED, F. R. (1961): *Crystallographic Computations. Part I: Generalized Structure Factor Program for the Basic IBM 650 Computer* (Report No. 6333); *Part II: Differential Synthesis Program for the Basic IBM 650 Computer* (Report No. 6478), National Research Council, Ottawa.

BACHMANN, H. G., & BARNES, W. H. (1961): Bonding in the trigonal bipyramidal coordination polyhedra of V_2O_5 and of certain other structures containing pentavalent vanadium, *Zeits. Krist.*, **115**, 215–230.

BACHMANN, H. G., AHMED, F. R., & BARNES, W. H. (1961): The crystal structure of vanadium pentoxide, *Zeits. Krist.*, **115**, 110–131.

BARNES, W. H., (1955): "Hewettite" and "metahewettite", *Am. Mineral.*, **40**, 689–691.

BARNES, W. H., & QURASHI, M. M. (1952): Unit cell and space group data for certain vanadium minerals, *Am. Mineral.*, **37**, 407–422.

BOOTH, A. D. (1946): The accuracy of atomic co-ordinates derived from Fourier series in *x*-ray structure analysis, *Proc. Roy. Soc.* (A) **188**, 77–92.

CRUICKSHANK, D. W. J. (1960): The required precision of intensity measurements for single-crystal analysis, *Acta Cryst.*, **13**, 774–777.

DONNAY, J. D. H., & NOWACKI, W. (1954): Crystal Data, *Geol. Soc. America, Mem.* **60**, New York.

FOSHAG, W. F., & HESS, F. L. (1927): Rossite and metarossite; two new vanadates from Colorado, *Proc. U.S. Nat. Museum*, **72**, art. 11.

FREEMAN, A. J. (1959): Atomic scattering factors for spherical and aspherical charge distributions, *Acta Cryst.*, **12**, 261–271.

FURNAS, T. C. (1957): *Single Crystal Orienter Instruction Manual*, General Electric, Milwaukee.

HANSON, A. W., & AHMED, F. R. (1958): The crystal structure and absolute configuration of the monoclinic form of *d*-methadone hydrobromide, *Acta Cryst.*, **11**, 724–728.

International Tables for X-ray Crystallography (1959): vol. II, Kynoch, Birmingham.

KELSEY, C. H., & BARNES, W. H. (1960): The crystal structure of metarossite, *Can. Mineral.*, **6**, 448–466.

——— (1961): *ibid.*, 697.

LIPSON, H., & COCHRAN, W. (1953): *The Crystalline State*, vol. III, *The Determination of Crystal Structures*, Bell, London.

QURASHI, M. M. (1962): The polymorphism and hydration characteristics of hewettite and metahewettite, *Can. Mineral.*, **6**, 647–662.

QURASHI, M. M., & BARNES, W. H. (1963): The structures of the minerals of the descloizite and adelite groups, IV: descloizite and conichalcite (part 2), the structure of conichalcite, *Can. Mineral.*, **7**, 561–577.

Manuscript received July 9, 1962